Received: 7 July 2020 | Revised: 7 September 2020 | Accepted: 13 October 2020

DOI: 10.1002/eom2.12062

REVIEW

EcoMat FUNCTIONAL MATERIALS FOR GREEN ENERGY AND ENVIRONMENT WILEY

Material choices for triboelectric nanogenerators: A critical review

Renyun Zhang | **Håkan Olin**

Department of Natural Sciences, Mid Sweden University, SE, Sundsvall, Sweden

Correspondence
Renyun Zhang, Department of Natural Sciences, Mid Sweden University, SE 85170 Sundsvall, Sweden.
Email: renyun.zhang@miun.se

Funding information
Energimyndigheten; European Regional Development Fund; Stiftelsen Promobilia

Abstract

A triboelectric nanogenerator (TENG) is a novel technology with applications in many areas, including energy harvesting, self-powered sensing, medication, and electronics. The materials used as triboelectric layers are diverse and include polymers, metals, and inorganic materials. The most commonly used materials are dielectric polymers such as PTFE, FEP, PDMS, and Kapton. Green materials, such as cellulose-based materials, have recently gained increasing interest, and the performance of TENGs using cellulose materials has improved. The material choices are of great importance for TENGs since the triboelectric effects of the materials are fundamental for TENGs. To design a TENG for a particular application, several parameters need to be considered, such as power density, stability, flexibility, and sustainability. This critical review will summarize and evaluate the material choices for TENGs in different applications.

KEYWORDS

electrostatic induction, material choices, triboelectric nanogenerators

1 | BACKGROUND

1.1 | Triboelectrification and TENGs

Triboelectrification, or contact electrification, is a physical phenomenon that describes the electron transfer between surfaces when physical contact occurs. Such a phenomenon was discovered 2600 years ago, while the mechanisms are still debated. Models such as the band structure model,[1] molecular orbital,[2] and electron-cloud-potential-well[3] models have been developed to describe the physical process. The band structure model,[1] the energy difference between the Fermi level of a metal and the valence band of a dielectric (if the dielectric can be presented with a band structure) will drive the transport of electrons. However, such a model meets challenges when the contact electrification happens between two dielectric materials that do not have well-specified band structures. The electron-cloud-potential-well model could explain the process better in this case. In this model, the electrons are in wells with different energy levels. One atom in a dielectric material has more occupied energy levels and the electrons in the highest level intend to flow the contacting atom from the other dielectric material. In the molecular orbital model, instead of using conduction and valence band that adopted from semiconductor, LUMO (the lowest unoccupied molecular orbital) and HOMO (the highest occupied molecular orbital) are utilized. The difference between the neutral level of the surface states of the two dielectrics drive the movement of the electrons.

Despite different theories have been developed to explain the electron transfer during a contact electrification process. It is still remaining to be studies because of the diverse choice of triboelectric materials.[4]

Despite the long history, the triboelectrification phenomenon was not widely utilized until 2012, when the first TENG was reported.[5] Lately, different TENGs have been invented that can categorized by four fundamental operation modes.[6] Applications of TENGs ranging from energy harvesting,[4] sensors,[7] implantable electronics,[8-11] and so forth. Reviews articles[6,7,12-15] on the TENGs with different focuses have been published in the past several years, showing the great success of the researches.

In a TENG, there is always a pair of triboelectric materials with different charge affinities that are employed to generate charges. Theoretically, to generate more charges or obtain a higher output from the TENG, a significant difference in the charge affinities[16] of the two materials is preferred. However, in practice, the two materials with the highest difference in charge affinity are not selected. The reason is that the triboelectrification between two materials is based not only on their chemical compositions but also on other physical features, such as the elasticity, friction, and surface topographical structure.[17] Moreover, based on the different purposes of applications, there are different requests of the materials other than the high triboelectric properties. Therefore, it is not fair to compare the advantages and disadvantages of different triboelectric materials without having the same applications. Some materials are excellent for energy harvesting, while others are better in sensing applications.

1.2 | Triboelectric series

The triboelectric effects of materials are usually represented by their surface charge density after undergoing a triboelectrification process with a reference material. The triboelectrification process can be a contact/separation process or a sliding process. Different triboelectrification processes may lead to different surface charge densities for the same material. However, in all the processes, PTFE is always one of the strongest electron accepting materials. Therefore, in most of the current studies of TENGs, PTFE is popularly used.

Due to the chemical compositions of the materials (assuming atomic flat surfaces), their affinities to positive and negative charges are different. By sorting the charge densities and affinities, a triboelectric series of materials has been constructed based on their charge densities after triboelectrification processes. The first triboelectric series was published by a Swedish physicist, Johan Carl Wilcke,[18] in 1757. Despite the long history of triboelectric series, most of the series that are being built currently are still based on qualitative data. In 2019, Wang's group at the Georgia Institute of Technology developed a new method[19] that can quantify the triboelectric charge density (TECD) of different materials based on their triboelectrification with mercury operating with the contact-separation mode. A new triboelectric series was built based on their TECDs measured after triboelectrification processes. Such a series is more reliable because of the precise control of the triboelectrification processes. Lately, another triboelectric series[20] based on the sliding mode has been reported with quantified charge density.

1.3 | Displacement current of TENGs

The displacement current is one of the most important parameters of TENGs that directly influence the output of the TENGs. The displacement current generated in a TENG is different from the one the presented in the Maxwell equations. In the Maxwell equations, the electric displacement vector, $D = \varepsilon_0 E + P$,where E is the electric field and P *is* the polarization vector. Here, the P is induced by an external electric field. However, in TENGs, the surface charges that generated are independent of the external electric field.[21] Therefore, a new term needs to be added and the displacement vector could be written as $D = \varepsilon_0 E + P + P_s$. The displacement current density of a TENG could then (J_D) be expressed as

$$J_D = \frac{\partial D}{\partial t} + \frac{\partial P_s}{\partial t} = \varepsilon \frac{\partial E}{\partial t} + \frac{\partial P_s}{\partial t} \tag{1}$$

The current density in the short-circuit case can be calculated by[22]

$$J_D = \sigma_T \frac{dH}{dt} \frac{d_1\varepsilon_0/\varepsilon_1 + d_2\varepsilon_0/\varepsilon_2}{\left(d_1\varepsilon_0/\varepsilon_1 + d_2\varepsilon_0/\varepsilon_2 + z\right)^2} + \frac{d\sigma_T}{dt} \frac{H}{d_1\varepsilon_0/\varepsilon_1 + d_2\varepsilon_0/\varepsilon_2 + z} \tag{2}$$

where σ_T is the surface charge density, H is a function of time, dH/dt represents the contact/separation of the two media in TENGs, d_1 and d_2 are the thicknesses of the two media, ε_0 is the vacuum permittivity, ε_1 and ε_2 are the permittivity of the two media, and z is the gap between the two triboelectric layers. The second term in the equation drops to a neglectable level after about 10 cycles when the surface charge density was built up. Therefore, Equation (1) can be rewritten as

$$J_D \approx \sigma_T \frac{dH}{dt} \frac{d_1\varepsilon_0/\varepsilon_1 + d_2\varepsilon_0/\varepsilon_2}{(d_1\varepsilon_0/\varepsilon_1 + d_2\varepsilon_0/\varepsilon_2 + z)^2} \quad (3)$$

Based on this equation, the output current, I, for a TENG with an area of A, can be estimated by equation

$$I \approx A\sigma_T \frac{dH}{dt} \frac{d_1\varepsilon_0/\varepsilon_1 + d_2\varepsilon_0/\varepsilon_2}{(d_1\varepsilon_0/\varepsilon_1 + d_2\varepsilon_0/\varepsilon_2 + z)^2} \quad (4)$$

Equations (2) and (3) show that the current density is a function of several parameters, where the surface charge density (σ_T) and the dielectric constant (ε_1, ε_2) are two of the most important parameters. The dielectric constants of the material pair in a TENG are determined by their chemical compositions, while the surface charge density is a result of several factors, such as the chemical and physical properties and the surface structure.

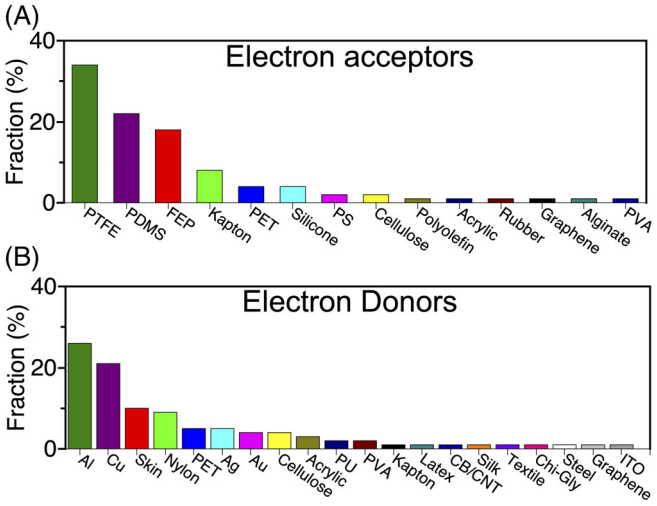

FIGURE 1 Fraction (%) of the electron acceptor, A, and donor, B, materials used in 100 randomly selected articles from 2012 to 2020. Cellulose in the figures represents materials made of cellulose fibers, such as paper and cellulose nanofibrils

2 | CURRENT MATERIAL CHOICES OF TENGS

2.1 | Summary of the material choices from 100 articles

The nature of triboelectrification is electron transfer between two materials in physical contact. The direction of the electron transfer depends on the difference in the electron affinities of the two materials. The one with a higher electron affinity will attract electrons from the other, making it an electron acceptor. The other one that loses electrons is therefore an electron donor. Generally, the donor and acceptor can be identified by their order in the triboelectric series. In this section, we summarize the current material choices for TENGs from 100 randomly selected articles.

Figure 1 shows the fraction of different materials used as either electron acceptors or donors. A total of 14 different electron acceptor materials (Figure 1A) were observed in the 100 articles. Polytetrafluoroethylene (PTFE),[9,10,23-55] polydimethyl-siloxane (PDMS),[56-77] fluorinated ethylene propylene (FEP),[33,78-95] and Kapton[5,33,96-101] are the most used electron acceptors. Among the 100 reports, 34% use PTFE as a triboelectric layer, while the percentages for PDMS and FEP are 22% and 18%, respectively. Other materials, such as polyvinylidene fluoride (PVDF),[102] polyolefin,[103] polystyrene (PS), [104,105] polyester (PET),[106-109] silicone,[110-113] bacterial nanocellulose (BNC),[114] alginate sodium,[115] nitrocellulose,[116] graphene,[117] acrylics,[108] rubber,[118] and polyvinyl alcohol (PVA),[115,119] have also been used in different studies.

For electron donor materials (Figure 1B), a total of 20 different materials have been found in the articles. Al,[23,25,26,28,29,32,35,40,41,43-45,47,53,54,60,65,69,74,77,78,83,89-91,99,103] Cu,[30,33,34,39,46,49,52,58,64,80,81,84-86,93-95,98,100,102,114] skin,[9,10,57,59,61,62,70,73,111,113] and nylon[24,38,50,72,97,104,107,108,118] are mostly used, and the percentages are 26%, 20%, 10%, and 8%, respectively. In addition, PET,[5,51,71,112,117] acrylics (PMMA),[88,96,108] polyurethane (PU),[31,68] Au,[48,67,76,92] Kapton,[27] cellulose (nanofibrils,[63,79] wood,[36] and paper[116]), indium-tin-oxide (ITO),[106] latex,[82] carbon black/carbon nanotubes (2:1),[110] textile,[37] graphene,[66] chitosan-glycerol,[42] silk,[101] PVA,[115,119] and steel[55] are also used as electron donors.

Interestingly, metal films, such Al, Cu, Ag, and Au, are widely used as both triboelectric layers and electrodes. Such a trend of using metal films is different from common sense that two materials with as different as possible charge affinities are preferred. The reason for these choices of triboelectric materials will be discussed below.

Figure 2 shows a network of how the electron acceptors and donors are paired in the 100 articles. PTFE is paired with 14 donors, PDMS is paired with 10 donors, FEP and Kapton are paired with 6 donors, and PET, silicone, PS, and cellulose (different cellulose materials are all counted as cellulose) are paired with 4, 3, 2, and 2 donors, respectively.

The selection of electron acceptor materials in the articles follows the trend of the triboelectric series, where the most negative materials, such as PTFE, PDMS, and FEP, are frequently used. Other materials, such as Kapton, PET, and silicone, are also utilized but are less popular than those above because their charge affinities are weaker.

In addition to the abovementioned triboelectric materials that have proven effects, other materials, such as

green materials, functionalized materials, and inorganic materials, have attracted much interest.

Recently, cellulose materials have gained increasing attention due to their sustainability and mass production capacity. Different cellulose materials, such as nano- and microcellulose,[63,79] regenerated cellulose, and modified cellulose,[120] have been applied in TENGs. The output power density of cellulose-based TENGs has recently improved very quickly as more efforts have been made.

Chemical modification of engineering polymers[17] has attracted interest because the modification can tune the surface triboelectricity, which can boost the output of the TENGs. This approach has great importance in future studies since it offers a way to tune the triboelectric effect of materials. However, we still know very little about the mechanisms by which the modification influences charge generation. There is a need for more efforts to address this issue.

Inorganic triboelectric materials, such as 2D materials such as graphene,[117] MoS_2,[121] and WS_2,[122] have also gained interest. The electron transfer mechanisms of these materials are much clearer than those of other polymers. However, research on these materials is still limited because of the difficulty in making large-area single crystalline films of these materials.

2.2 | Specific material choices

There are four fundamental modes of operation for TENGs[6]: single electrode mode, contact-separation mode, lateral sliding mode, and freestanding triboelectric layer mode. The triboelectric materials have vertical contact in the first two modes, and the material choices are quite broad. Almost all the currently used materials can be used in these two modes.

Different from the first two modes, the last two modes have a specific requirement for the materials, that is, a low coefficient of friction. The sliding of materials on each other can wear the materials down if they have high coefficients of friction. This specific requirement limits the material choices for the lateral sliding mode and the freestanding triboelectric layer mode. PTFE and FEP are mostly used as electron acceptors in these two modes because of their low coefficients of friction. Examples can be found in articles where material pairs such as PTFE-nylon,[38] PTFE-Al,[23,25,26] FEP-Cu,[85,86] FEP-Al,[78,90,123] and PTFE-skin[124] are used.

3 | EVALUATION OF THE MATERIAL CHOICES FOR TENGS

In addition to the triboelectric materials that have been reviewed above, more materials have been studied. However, few studies state why the pair of materials is used. In principle, the two triboelectric materials should have as large a difference in charge affinity as possible or be as far from each other in the triboelectric series as possible. If one follows this principle, then the pair of PTFE and nylon should be one of the best pairs. However, only three studies used the PTFE/nylon pair among the 100 articles. That said, there are more factors that can influence the output or performance of a TENG.

A theoretical explanation can be found in Equation (3). We can divide the equation into three parts (Figure 3). The first part (P_1), the surface charge density σ_T, is a result of different factors, such as the chemical compositions of the materials, the interaction of the materials during contact and the mechanical properties of the materials, such as the elasticity (for contact-separation mode) and friction (for sliding mode and freestanding triboelectric layer mode). The middle part (P_2), dH/dt, describes the operation of the TENG devices, where the contact or sliding speeds play important roles. The last part (P_3) describes the electrostatic induction, which is one of two fundamental physics ideas behind TENGs. In this part, the permittivity has a high impact on the induced charges on the back electrodes. Generally, P_1 represents the triboelectric effect, P_2 represents the operation of the TENG devices, and P_3 represents electrostatic induction.

In the discussion below, P_3 will be the focus, where

$$P_3 = \frac{d_1\varepsilon_0/\varepsilon_1 + d_2\varepsilon_0/\varepsilon_2}{\left(d_1\varepsilon_0/\varepsilon_1 + d_2\varepsilon_0/\varepsilon_2 + z\right)^2} \tag{5}$$

3.1 | Electron donors

3.1.1 | Metals

Based on Equation (5), we can discuss why metals are widely used in TENGs. In the case of metals, the term $d_2\varepsilon_0/\varepsilon_2$ equals 0 since d_2 is 0. Therefore, Equation (3) becomes

$$J_D \approx \sigma_T \frac{dH}{dt} \frac{d_1\varepsilon_0/\varepsilon_1}{\left(d_1\varepsilon_0/\varepsilon_1 + z\right)^2} \tag{6}$$

and

$$P_3' = \frac{d_1\varepsilon_0/\varepsilon_1}{\left(d_1\varepsilon_0/\varepsilon_1 + z\right)^2} \tag{7}$$

Even if we assume that there is a thin metallic triboelectric layer on the metal surface, Equation (6) still

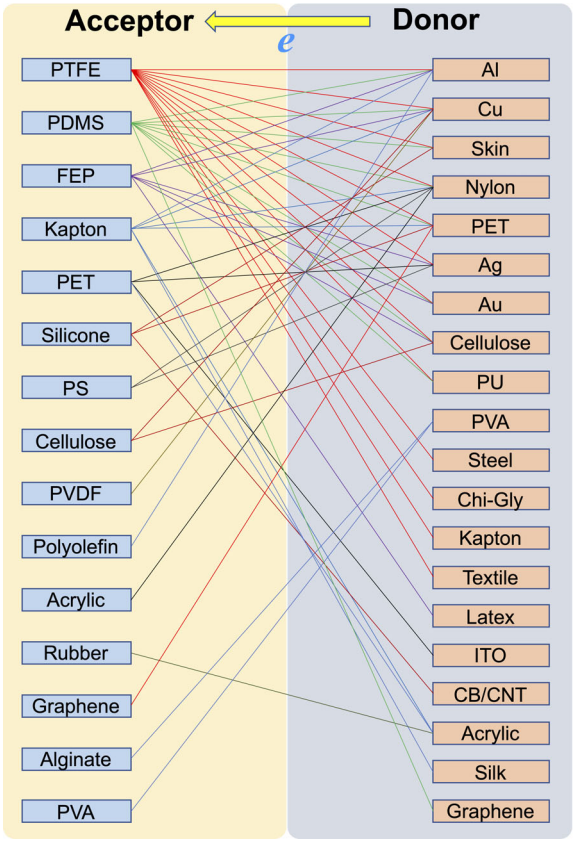

FIGURE 2 Network showing how the electron acceptors and donors are paired in the selected 100 articles

works. The reason is that the relative permittivity of metals, such as Cu, is very high (>250 000). With such a high value, the term $(d_2\varepsilon_0/\varepsilon_2) \approx 0$, and thus, Equation (6) is still valid.

In the case of having metals as electron donors, the electrical induction effect in the equation will highly depend on the gap distance. Figure 4A shows plots of the values of P_3' for different materials vs the gap distance when using metals as electron donors. The plots indicate that the electron acceptor materials with smaller permittivities would have more substantial electrostatic induction effects (assuming the materials have the same thickness and surface geometry). However, the differences among the material pairs are not significant.

Figure 4B shows the plot of P_3 in Equation (5) when pairing PTFE with metals and other triboelectric layers. The thicknesses of the layers are set as 0.1 mm. Significant differences among the material pairs are found in the figure. The PTFE-metal pair has the highest value, which could be approximately twice that of the PTFE-cellulose pair at a gap distance of 0.05 mm.

The above results indicate that metals are preferred as electron donors in triboelectric material pairs based on the electrostatic induction part in Equation (3). However,

$$J_D \approx \underbrace{\left[\sigma_T\right]}_{(P_1)} \underbrace{\left[\frac{dH}{dt}\right]}_{(P_2)\ \text{Device}} \underbrace{\left[\frac{d_1\,\varepsilon_0/\varepsilon_1 + d_2\,\varepsilon_0/\varepsilon_2}{(d_1\,\varepsilon_0/\varepsilon_1 + d_2\,\varepsilon_0/\varepsilon_2 + z)^2}\right]}_{(P_3)}$$

Triboelectric effect — Electrostatic induction

FIGURE 3 Deconstructed Equation (1), showing the three parts of the triboelectric effect (P_1), device (P_2), and electrostatic induction (P_3)

the electrostatic induction part is just one of the three parts that contribute to the current density, and how much it can contribute is unclear. More studies should be performed to determine which part is of greater importance for the future selection of material pairs.

3.1.2 | Carbon-based electron donors

Carbon materials, such as carbon black,[110] graphene,[66] and graphite,[125] could act similar to metals because of their good electrical conductivities. The limitation of these materials is that they are soft, and small pieces of the materials can fall off and become stacked on the surface of the counter triboelectric layer. An advantage of the materials may also arise from the softness since the softness can allow the surface structure to adjust to fit the counter surface, maximizing the contact area.

3.2 | Electron acceptors

Different from the diverse choices of electron donor materials in the reported papers, the electron acceptor materials that are popularly used are PTFE,[38] FEP,[78] and PDMS.[126] Other polymers, such as PC,[97] PS,[97] and ABS,[19] that have TECDs close to that of PDMS are not widely used. There is no doubt that researchers have tested more polymers in TENGs. However, their less popularity implies that there are some unknown factors limiting the output from TENGs made of these polymers.

A reason might be that the triboelectric effects of these polymers against commonly used electron donors are not as strong as those against mercury used to test the TECD. We can take PET as an example to discuss the differences. The TECD value[19] of PET against mercury is −101.48 μC/m^2, which is very negative and close to that of PTFE (−113.06 μC/m^2). However, in another test[20] where PET was laterally slid against a copper board, the charge density was −1.09 μC/m^2, which is far below that of PTFE (−27.5 μC/m^2). A similar phenomenon could also be found for PC and ABS. The real reason for the

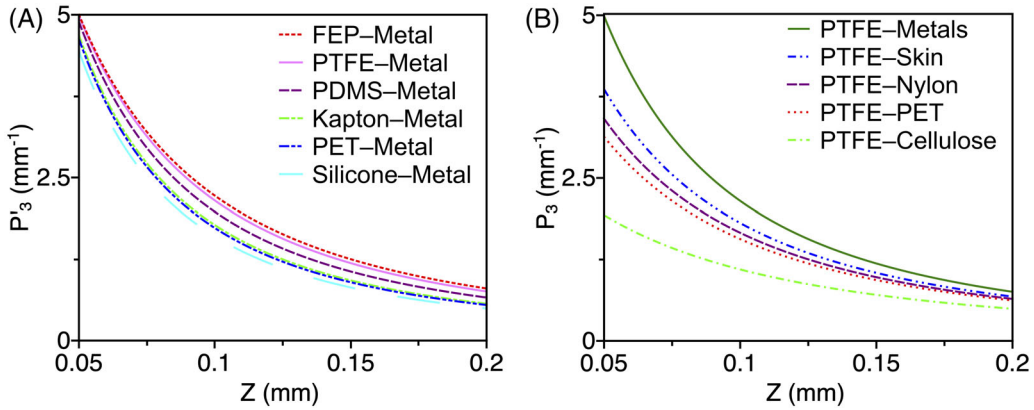

FIGURE 4 A, Plots of the value of P_3' in Equation (7) vs the gap distance for different material pairs using metals as electron donors. B, Plots of the value of P_3 in Equation (5) vs the gap distance for different material pairs using PTFE as the electron acceptor

phenomena has not yet been explored. However, an argument can be raised based on Equation (3). As we have noted above, P_1 in the equation, the surface charge density (σ_T), represents the triboelectric effect in the TENGs. This triboelectric effect is a result of several parameters: the charge affinity, the interaction between the triboelectric layers, the mode of interaction (sliding or contact-separation), the mechanical properties, the surface geometry, and so forth. The charge affinity is based on the chemical compositions of the materials, which determine their abilities to attract electrons. The chemical structures of the materials will determine their polarities, which are of great importance in triboelectrification processes. The interaction between the triboelectric layers is based on the surface energies of the materials and will basically determine the energy difference at the interface that guides the electron transfer. The mode of the interaction (sliding or contact-separation) has an impact on the effective contact area of the interface. Other side effects, such as the heat generated in the sliding mode, will also have an impact on the electron transfer. The difference in the charge density of PET mentioned above might be caused by the different operation modes. The interaction with mercury is the contact-separation mode, while the interaction with the copper board is the sliding mode. The mechanical properties of the materials determine how much shape deformation occurs during contact or the friction on the interface. The surface geometry determines the effective contact area and the distribution of the surface potential. However, it is not clear how these parameters act during triboelectrification. Theoretical models are highly needed to predict the contributions of these parameters.

3.3 | Dual usage materials

In Figures 1 and 2, we can see that some materials, such as PET,[106-109,112,117] PVA[115,119] and cellulose,[63,79,114] have been used as both electron acceptors and donors. It should be stated that not exactly the same material was used as an electron acceptor or donor. For example, the PVA[115,119] that we cited here is negatively ionized as an acceptor and positively ionized as a donor. For cellulose, there are different types of cellulose with different doping or functionalization. One possibility that we can see from these studies is that we can utilize different techniques such as surface modification/functionalization[115,119] to change the triboelectric properties of a material. By tuning the properties of materials, we can fabricate TENGs with higher performance. This is of great importance for the future development of new triboelectric materials.

Among these dual usage materials, cellulose could have a great future because of its sustainability, mass production, and chemical feasibility. There is a great chance to tune the triboelectric properties of cellulose by chemical doping or functionalization. The rising attention that cellulose-based TENGs has attracted is indicated by the recent increase in publications.[125]

4 | FUTURE PROSPECTS

Since the first TENG was invented in 2012,[5] TENGs have attracted increasing interest due to their broad applications and diverse material choices. Many devices have been developed for use in energy harvesting, sensing, human-machine interaction, medication, and so forth. Many materials have been used for different purposes. However, some fundamental and practical issues remain for future studies.

4.1 | Surface charge density (σ_T)

Equation (3), which was developed by Wang in 2019,[22] describes the correlations of the displacement current

density with the triboelectric effect of the materials, the electrostatic induction, and the operation of the TENG. The electrostatic induction and the operation of the TENG in the equation can be quantitatively described, while there are limited studies that aim to theoretically predict the surface charge density (σ_T) in addition to the experimental approaches. We can draw the conclusion that fluoropolymers, such as PTFE, FEP, and PFA, generally have the highest negative charge affinities, which is due to the higher content of fluorine, which has the second highest electron affinity among all the elements (chlorine has the highest). Theoretical studies are highly required to determine how the chemical structure correlates with the charge affinities of different materials. With this understanding, one can move forward in describing the surface charge density (σ_T) quantitatively.

4.2 | New triboelectric materials

Currently, most of the triboelectric materials used are commercial polymers with known triboelectric charge density, dielectric properties, and other relevant parameters, such as the coefficient of friction. However, these materials are just a small portion of the materials that exist. There are more materials that could possibly perform better. For example, the TECD of cellulose acetate[19] was not determined until 2019 because cellulose materials are usually thought to not have a strong triboelectric effect. The group at Mid Sweden University recently found that regenerated cellulose could have an excellent triboelectric effect,[125] and the TECD is among the most positive ones for the materials that have been tested.

Beside cellulose, there are other biopolymers[127] that could be used in TENGs such as chitosan,[128,129] lignin,[130] fish gelatin[131] and fabricated nanofiber.[132] Chitosan is a natural biopolymer that widely exists in marine crustacean shells. The application of such material in TENGs[128,129] could have great impact considering of the huge amount of sea creature shells produced in the food industry every year. Lignin is widely existing in trees and plants that can easily form thin films for using in TENGs, however, studies are limited. One unique characteristic is that lignin can be easily modified to tune the chemical and physical properties. With such kind of modification, one can achieve higher positive or negative charge affinities that can boost the performances of the TENGs.

Tuning the triboelectric properties by doping[133] or modification[120] of the polymers such as cellulose[134,135] could enhance their triboelectric effects. More efforts need to be made in this area since doping and modification may allow us to design materials with desired properties. Such an approach will also help in understanding how the chemical structures correlate with the triboelectric effects. There are possibilities to quantify the doping and modification, which affords chances to describe the correlation quantitatively.

Inorganic materials are less studied in TENGs[122,136] and could be the next hot topic. Inorganic materials can tolerate some extreme conditions better than polymers, such as high temperature and high pressure. Inorganic materials can also survive longer than polymers under sunshine because the oxidation of polymer occurs much faster. There are studies that have tested the triboelectric effect of 2D materials[122] and metallic oxides,[136] while more efforts could be made for inorganic materials.

Composite materials also need more attention because they can combine the advantages of their component materials.[137-139] Composites can have better triboelectric effects or better mechanical properties that could significantly extend the lifetime of the TENG. Moreover, by utilizing the antibacterial property of a component material in a composite, a TENG can have other functions, such as antibacterial effects.[137]

5 | CONCLUSION

Triboelectrification can occur at any interface where two materials come into physical contact. For this reason, many materials have the possibility to be used in TENGs. Many materials have been tested for their triboelectric effects and applied in TENGs. Fluoropolymers, such as PTFE and FEP, are the most popularly used triboelectric materials as electron acceptors in TENGs, especially for TENGs operated in the lateral sliding mode and free-standing triboelectric layer mode. Metal films, such as Al and Cu films, are widely used as electron donors. The reasons why metals are popular can be quantitatively explained by using the recently developed equation, where the use of metals can enhance the electrostatic induction in the TENGs.

Despite the fact that great success has been achieved in the selection of triboelectric materials, many other materials remain unexplored. New materials (such as green materials), functionalized materials, inorganic materials, and composite materials are highly demanded to extend the usage of TENGs.

In addition to the development of materials, there is also a need for a better understanding of the triboelectric effect of the materials, for example, how the charge density correlates with the chemical composition of the materials and how the charge density correlates with the interaction of the triboelectric layers. With this understanding, we might be able to explain the triboelectric charge density of different materials quantitatively.

In summary, this review summarized the material choices for TENGs, critically reviewed the material choices, and evaluated the choices using recently developed theory. Theoretical evaluations of the material choices have been made based on the recently developed theory. The critical review affords new findings on why metals are popularly in TENGs and what kinds of triboelectric material pairs could contribute more to the displacement current density if P_3 in Equation (3) is focusing. However, P_1 in Equation (3) should be considered when estimating the total displacement current density. Besides, future prospects have also been discussed, which might lead to the development of new triboelectric materials.

ACKNOWLEDGMENTS

This work is financially supported by the European Regional Development Fund, the Energy Agency of Sweden, Promobilia Stiftelsen, Region Västernorrland, Sundsvalls Kommun, Timrå Kommun, and Härnösands Kommun.

ORCID

Renyun Zhang https://orcid.org/0000-0003-2873-7875

REFERENCES

1. Zhou YS, Wang S, Yang Y, et al. Manipulating nanoscale contact electrification by an applied electric field. *Nano Lett*. 2014;14(3):1567-1572. https://doi.org/10.1021/nl404819w.
2. Xu C, Zhang B, Wang AC, et al. Contact-electrification between two identical materials: curvature effect. *ACS Nano*. 2019;13:2034-2041. https://doi.org/10.1021/acsnano.8b08533.
3. Xu C, Wang AC, Zou H, et al. Raising the working temperature of a triboelectric nanogenerator by quenching down electron thermionic emission in contact-electrification. *Adv Mater*. 2018;30(38):1803968. https://doi.org/10.1002/adma.201803968.
4. Zi Y, Wang ZL. Nanogenerators: an emerging technology towards nanoenergy. *APL Mater*. 2017;5(7):074103. https://doi.org/10.1063/1.4977208.
5. Fan F-R, Tian Z-Q, Wang ZL. Flexible triboelectric generator. *Nano Energy*. 2012;1(2):328-334. https://doi.org/10.1016/j.nanoen.2012.01.004.
6. Wang ZL. Triboelectric nanogenerators as new energy technology and self-powered sensors – principles, problems and perspectives. *Faraday Discuss*. 2014;176:447-458. https://doi.org/10.1039/C4FD00159A.
7. Sun J, Yang A, Zhao C, Liu F, Li Z. Recent progress of nanogenerators acting as biomedical sensors in vivo. *Sci Bull*. 2019;64(18):1336-1347. https://doi.org/10.1016/j.scib.2019.07.001.
8. Shi B, Liu Z, Zheng Q, et al. Body-integrated self-powered system for wearable and implantable applications. *ACS Nano*. 2019;13(5):6017-6024. https://doi.org/10.1021/acsnano.9b02233.
9. Jiang D, Shi B, Ouyang H, et al. A 25-year bibliometric study of implantable energy harvesters and self-powered implantable medical electronics researches. *Mater Today Energy*. 2020;16:100386. https://doi.org/10.1016/j.mtener.2020.100386.
10. Jiang D, Shi B, Ouyang H, Fan Y, Wang ZL, Li Z. Emerging implantable energy harvesters and self-powered implantable medical electronics. *ACS Nano*. 2020;14(6):6436-6448. https://doi.org/10.1021/acsnano.9b08268.
11. Zheng Q, Zou Y, Zhang Y, et al. Biodegradable triboelectric nanogenerator as a life-time designed implantable power source. *Sci Adv*. 2016;2(3):1-10. https://doi.org/10.1126/sciadv.1501478.
12. Wang ZL, Chen J, Lin L. Progress in triboelectric nanogenerators as a new energy technology and self-powered sensors. *Energy Environ Sci*. 2015;8(8):2250-2282. https://doi.org/10.1039/C5EE01532D.
13. Zhang C, Wang ZL. Tribotronics—a new field by coupling triboelectricity and semiconductor. *Nano Today*. 2016;11(4):521-536. https://doi.org/10.1016/j.nantod.2016.07.004.
14. Yi F, Zhang Z, Kang Z, Liao Q, Zhang Y. Recent advances in triboelectric nanogenerator-based health monitoring. *Adv Funct Mater*. 2019;29(41):1808849. https://doi.org/10.1002/adfm.201808849.
15. Lee JW, Ye BU, Baik JM. Research update: recent progress in the development of effective dielectrics for high-output triboelectric nanogenerator. *APL Mater*. 2017;5(7):073802. https://doi.org/10.1063/1.4979306.
16. Chen X, Song Y, Chen H, Zhang J, Zhang H. An ultrathin stretchable triboelectric nanogenerator with coplanar electrode for energy harvesting and gesture sensing. *J Mater Chem A*. 2017;5(24):12361-12368. https://doi.org/10.1039/C7TA03092D.
17. Chen J, Wang ZL. Reviving vibration energy harvesting and self-powered sensing by a triboelectric nanogenerator. *Dent J*. 2017;1(3):480-521. https://doi.org/10.1016/j.joule.2017.09.004.
18. Wang ZL, Lin L, Chen J, Niu S, Zi Y. Triboelectric nanogenerators. *Springer International Publishing*. Cham: Springer. 2016. https://doi.org/10.1007/978-3-319-40039-6.
19. Zou H, Zhang Y, Guo L, et al. Quantifying the triboelectric series. *Nat Commun*. 2019;10(1):1427. https://doi.org/10.1038/s41467-019-09461-x.
20. Liu S, Zheng W, Yang B, Tao X. Triboelectric charge density of porous and deformable fabrics made from polymer fibers. *Nano Energy*. 2018;53:383-390. https://doi.org/10.1016/j.nanoen.2018.08.071.
21. Wang ZL. On the first principle theory of nanogenerators from Maxwell's equations. *Nano Energy*. 2020;68:104272. https://doi.org/10.1016/j.nanoen.2019.104272.

22. Wang ZL. On the first principle theory of nanogenerators from Maxwell's equations. *Nano Energy*. 2019;68:104272. https://doi.org/10.1016/j.nanoen.2019.104272.
23. Zhu G, Chen J, Liu Y, et al. Linear-grating triboelectric generator based on sliding electrification. *Nano Lett*. 2013;13(5):2282-2289. https://doi.org/10.1021/nl4008985.
24. Yang Y, Zhang H, Liu R, Wen X, Hou TC, Wang ZL. Fully enclosed triboelectric nanogenerators for applications in water and harsh environments. *Adv Energy Mater*. 2013;3(12):1563-1568. https://doi.org/10.1002/aenm.201300376.
25. Xie Y, Wang S, Lin L, et al. Rotary triboelectric nanogenerator based on a hybridized mechanism for harvesting wind energy. *ACS Nano*. 2013;7(8):7119-7125. https://doi.org/10.1021/nn402477h.
26. Tang W, Han CB, Zhang C, Wang ZL. Cover-sheet-based nanogenerator for charging mobile electronics using low-frequency body motion/vibration. *Nano Energy*. 2014;9:121-127. https://doi.org/10.1016/j.nanoen.2014.07.005.
27. Wang X, Wang S, Yang Y, Wang ZL. Hybridized electromagnetic-triboelectric nanogenerator for scavenging air-flow energy to sustainably power temperature sensors. *ACS Nano*. 2015;9(4):4553-4562. https://doi.org/10.1021/acsnano.5b01187.
28. Quan Z, Han CB, Jiang T, Wang ZL. Robust thin films-based triboelectric nanogenerator arrays for harvesting bidirectional wind energy. *Adv Energy Mater*. 2016;6(5):1501799. https://doi.org/10.1002/aenm.201501799.
29. Jeon SB, Kim S, Park SJ, et al. Self-powered electrocoagulation system driven by a wind energy harvesting triboelectric nanogenerator for decentralized water treatment. *Nano Energy*. 2016;28:288-295. https://doi.org/10.1016/j.nanoen.2016.08.051.
30. Lin Z, Chen J, Li X, et al. Triboelectric nanogenerator enabled body sensor network for self-powered human heart-rate monitoring. *ACS Nano*. 2017;11(9):8830-8837. https://doi.org/10.1021/acsnano.7b02975.
31. Zhang SL, Lai Y-C, He X, Liu R, Zi Y, Wang ZL. Auxetic foam-based contact-mode Triboelectric Nanogenerator with highly sensitive self-powered strain sensing capabilities to monitor human body movement. *Adv Funct Mater*. 2017;27(25):1606695. https://doi.org/10.1002/adfm.201606695.
32. He C, Zhu W, Chen B, et al. Smart floor with integrated triboelectric nanogenerator as energy harvester and motion sensor. *ACS Appl Mater Interfaces*. 2017;9(31):26126-26133. https://doi.org/10.1021/acsami.7b08526.
33. Xu M, Wang Y-C, Zhang SL, et al. An aeroelastic flutter based triboelectric nanogenerator as a self-powered active wind speed sensor in harsh environment. *Extrem Mech Lett*. 2017;15:122-129. https://doi.org/10.1016/j.eml.2017.07.005.
34. Guo H, Jia X, Liu L, Cao X, Wang N, Wang ZL. Freestanding triboelectric nanogenerator enables noncontact motion-tracking and positioning. *ACS Nano*. 2018;12(4):3461-3467. https://doi.org/10.1021/acsnano.8b00140.
35. Bian Y, Jiang T, Xiao T, et al. Triboelectric nanogenerator tree for harvesting wind energy and illuminating in subway tunnel. *Adv Mater Technol*. 2018;3(3):1700317. https://doi.org/10.1002/admt.201700317.
36. Luo J, Wang Z, Xu L, et al. Flexible and durable wood-based triboelectric nanogenerators for self-powered sensing in athletic big data analytics. *Nat Commun*. 2019;10(1):5147. https://doi.org/10.1038/s41467-019-13166-6.
37. Bae J, Lee J, Kim S, et al. Flutter-driven triboelectrification for harvesting wind energy. *Nat Commun*. 2014;5:4929. https://doi.org/10.1038/ncomms5929.
38. Wang S, Lin L, Xie Y, Jing Q, Niu S, Wang ZL. Sliding-triboelectric nanogenerators based on in-plane charge-separation mechanism. *Nano Lett*. 2013;13(5):2226-2233. https://doi.org/10.1021/nl400738p.
39. Wang S, Mu X, Wang X, Gu AY, Wang ZL, Yang Y. Elasto-aerodynamics-driven triboelectric nanogenerator for scavenging air-flow energy. *ACS Nano*. 2015;9(10):9554-9563. https://doi.org/10.1021/acsnano.5b04396.
40. Chen J, Yang J, Li Z, et al. Networks of triboelectric nanogenerators for harvesting water wave energy: a potential approach toward blue energy. *ACS Nano*. 2015;9(3):3324-3331. https://doi.org/10.1021/acsnano.5b00534.
41. Wang S, Mu X, Yang Y, Sun C, Gu AY, Wang ZL. Flow-driven triboelectric generator for directly powering a wireless sensor node. *Adv Mater*. 2015;27(2):240-248. https://doi.org/10.1002/adma.201403944.
42. Jao Y-T, Yang P-K, Chiu C-M, et al. A textile-based triboelectric nanogenerator with humidity-resistant output characteristic and its applications in self-powered healthcare sensors. *Nano Energy*. 2018;50:513-520. https://doi.org/10.1016/j.nanoen.2018.05.071.
43. Zhu G, Bai P, Chen J, Lin Wang Z. Power-generating shoe insole based on triboelectric nanogenerators for self-powered consumer electronics. *Nano Energy*. 2013;2(5):688-692. https://doi.org/10.1016/j.nanoen.2013.08.002.
44. Chen J, Zhu G, Yang W, et al. Harmonic-resonator-based triboelectric nanogenerator as a sustainable power source and a self-powered active vibration sensor. *Adv Mater*. 2013;25(42):6094-6099. https://doi.org/10.1002/adma.201302397.
45. Bai P, Zhu G, Lin Z-H, et al. Integrated multilayered triboelectric nanogenerator for harvesting biomechanical energy from human motions. *ACS Nano*. 2013;7(4):3713-3719. https://doi.org/10.1021/nn4007708.
46. Zhu G, Zhou YS, Bai P, et al. A shape-adaptive thin-film-based approach for 50% high-efficiency energy generation through micro-grating sliding electrification. *Adv Mater*. 2014;26(23):3788-3796. https://doi.org/10.1002/adma.201400021.
47. Yang J, Chen J, Liu Y, Yang W, Su Y, Wang ZL. Triboelectrification-based organic film Nanogenerator for acoustic energy harvesting and self-powered active acoustic sensing. *ACS Nano*. 2014;8(3):2649-2657. https://doi.org/10.1021/nn4063616.
48. Jung W-S, Kang M-G, Moon HG, et al. High output Piezo/Triboelectric hybrid generator. *Sci Rep*. 2015;5(1):9309. https://doi.org/10.1038/srep09309.
49. Fan X, Chen J, Yang J, Bai P, Li Z, Wang ZL. Ultrathin, Rollable, paper-based triboelectric nanogenerator for acoustic energy harvesting and self-powered sound recording. *ACS Nano*. 2015;9(4):4236-4243. https://doi.org/10.1021/acsnano.5b00618.
50. Yang J, Chen J, Su Y, et al. Eardrum-inspired active sensors for self-powered cardiovascular system characterization and throat-attached anti-interference voice recognition. *Adv Mater*. 2015;27(8):1316-1326. https://doi.org/10.1002/adma.201404794.

51. Guo H, Chen J, Leng Q, et al. Spiral-interdigital-electrode-based multifunctional device: dual-functional triboelectric generator and dual-functional self-powered sensor. *Nano Energy*. 2015;12:626-635. https://doi.org/10.1016/j.nanoen.2014.09.021.
52. Lee KY, Yoon H-J, Jiang T, et al. Fully packaged self-powered triboelectric pressure sensor using hemispheres-Array. *Adv Energy Mater*. 2016;6(11):1502566. https://doi.org/10.1002/aenm.201502566.
53. Zheng Q, Zhang H, Shi B, et al. In vivo self-powered wireless cardiac monitoring via implantable triboelectric nanogenerator. *ACS Nano*. 2016;10(7):6510-6518. https://doi.org/10.1021/acsnano.6b02693.
54. Ma Y, Zheng Q, Liu Y, et al. Self-powered, one-stop, and multifunctional implantable triboelectric active sensor for real-time biomedical monitoring. *Nano Lett*. 2016;16(10):6042-6051. https://doi.org/10.1021/acs.nanolett.6b01968.
55. Liu G, Chen J, Guo H, et al. Triboelectric nanogenerator based on magnetically induced retractable spring steel tapes for efficient energy harvesting of large amplitude motion. *Nano Res*. 2018;11(2):633-641. https://doi.org/10.1007/s12274-017-1668-2.
56. Lin L, Xie Y, Wang S, et al. Triboelectric active sensor Array for self-powered static and dynamic pressure detection and tactile imaging. *ACS Nano*. 2013;7(9):8266-8274. https://doi.org/10.1021/nn4037514.
57. Meng B, Cheng X, Zhang X, Han M, Liu W, Zhang H. Single-friction-surface triboelectric generator with human body conduit. *Appl Phys Lett*. 2014;104(10):103904. https://doi.org/10.1063/1.4868130.
58. Wen Z, Yeh M-H, Guo H, et al. Self-powered textile for wearable electronics by hybridizing fiber-shaped nanogenerators, solar cells, and supercapacitors. *Sci Adv*. 2016;2(10):e1600097. https://doi.org/10.1126/sciadv.1600097.
59. Dhakar L, Pitchappa P, Tay FEH, Lee C. An intelligent skin based self-powered finger motion sensor integrated with triboelectric nanogenerator. *Nano Energy*. 2016;19:532-540. https://doi.org/10.1016/j.nanoen.2015.04.020.
60. Dudem B, Huynh ND, Kim W, et al. Nanopillar-array architectured PDMS-based triboelectric nanogenerator integrated with a windmill model for effective wind energy harvesting. *Nano Energy*. 2017;42:269-281. https://doi.org/10.1016/j.nanoen.2017.10.040.
61. Sun J-G, Yang TN, Kuo I-S, Wu J-M, Wang C-Y, Chen L-J. A leaf-molded transparent triboelectric nanogenerator for smart multifunctional applications. *Nano Energy*. 2017;32:180-186. https://doi.org/10.1016/j.nanoen.2016.12.032.
62. Rasel MSU, Park J-Y. A sandpaper assisted micro-structured polydimethylsiloxane fabrication for human skin based triboelectric energy harvesting application. *Appl Energy*. 2017;206:150-158. https://doi.org/10.1016/j.apenergy.2017.07.109.
63. Qian C, Li L, Gao M, et al. All-printed 3D hierarchically structured cellulose aerogel based triboelectric nanogenerator for multi-functional sensors. *Nano Energy*. 2019;63:103885. https://doi.org/10.1016/j.nanoen.2019.103885.
64. Yang B, Tao X, Peng Z. Upper limits for output performance of contact-mode triboelectric nanogenerator systems. *Nano Energy*. 2019;57:66-73. https://doi.org/10.1016/j.nanoen.2018.12.013.
65. Zhang K, Wang X, Yang Y, Wang ZL. Hybridized electromagnetic–Triboelectric Nanogenerator for scavenging biomechanical energy for sustainably powering wearable electronics. *ACS Nano*. 2015;9(4):3521-3529. https://doi.org/10.1021/nn507455f.
66. Chandrashekar BN, Deng B, Smitha AS, et al. Roll-to-roll green transfer of CVD Graphene onto plastic for a transparent and flexible Triboelectric Nanogenerator. *Adv Mater*. 2015;27(35):5210-5216. https://doi.org/10.1002/adma.201502560.
67. Chun J, Ye BU, Lee JW, et al. Boosted output performance of triboelectric nanogenerator via electric double layer effect. *Nat Commun*. 2016;7:12985. https://doi.org/10.1038/ncomms12985.
68. Chen X, Miao L, Guo H, et al. Waterproof and stretchable triboelectric nanogenerator for biomechanical energy harvesting and self-powered sensing. *Appl Phys Lett*. 2018;112(20):203902. https://doi.org/10.1063/1.5028478.
69. Han M, Zhang X-S, Meng B, et al. R-shaped hybrid Nanogenerator with enhanced piezoelectricity. *ACS Nano*. 2013;7(10):8554-8560. https://doi.org/10.1021/nn404023v.
70. Yang Y, Zhang H, Z-HH L, et al. Human skin based triboelectric nanogenerators for harvesting biomechanical energy and as self-powered active tactile sensor system. *ACS Nano*. 2013;7(10):9213-9222. https://doi.org/10.1021/nn403838y.
71. Hou T-C, Yang Y, Zhang H, Chen J, Chen LJ, Lin Wang Z. Triboelectric nanogenerator built inside shoe insole for harvesting walking energy. *Nano Energy*. 2013;2(5):856-862. https://doi.org/10.1016/J.NANOEN.2013.03.001.
72. Li X, Lin Z-H, Cheng G, et al. 3D fiber-based hybrid Nanogenerator for energy harvesting and as a self-powered pressure sensor. *ACS Nano*. 2014;8(10):10674-10681. https://doi.org/10.1021/nn504243j.
73. Yang W, Chen J, Wen X, et al. Triboelectrification based motion sensor for human-machine interfacing. *ACS Appl Mater Interfaces*. 2014;6(10):7479-7484. https://doi.org/10.1021/am500864t.
74. Lee KY, Chun J, Lee J-H, et al. Hydrophobic sponge structure-based triboelectric nanogenerator. *Adv Mater*. 2014;26(29):5037-5042. https://doi.org/10.1002/adma.201401184.
75. Seung W, Gupta MK, Lee KY, et al. Nanopatterned textile-based wearable triboelectric nanogenerator. *ACS Nano*. 2015;9(4):3501-3509. https://doi.org/10.1021/nn507221f.
76. Kim KN, Chun J, Kim JW, et al. Highly stretchable 2D fabrics for wearable triboelectric nanogenerator under harsh environments. *ACS Nano*. 2015;9(6):6394-6400. https://doi.org/10.1021/acsnano.5b02010.
77. Feng H, Zhao C, Tan P, Liu R, Chen X, Li Z. Nanogenerator for biomedical applications. *Adv Healthc Mater*. 2018;7(10):1701298. https://doi.org/10.1002/adhm.201701298.
78. Xie Y, Wang S, Niu S, et al. Grating-structured freestanding triboelectric-layer nanogenerator for harvesting mechanical energy at 85% total conversion efficiency. *Adv Mater*. 2014;26(38):6599-6607. https://doi.org/10.1002/adma.201402428.
79. Yao C, Hernandez A, Yu Y, Cai Z, Wang X. Triboelectric nanogenerators and power-boards from cellulose nanofibrils and recycled materials. *Nano Energy*. 2016;30:103-108. https://doi.org/10.1016/j.nanoen.2016.09.036.
80. Yeh M-H, Guo H, Lin L, et al. Rolling friction enhanced freestanding Triboelectric Nanogenerators and their applications

in self-powered electrochemical recovery systems. *Adv Funct Mater*. 2016;26(7):1054-1062. https://doi.org/10.1002/adfm.201504396.

81. Zi Y, Guo H, Wen Z, Yeh M-H, Hu C, Wang ZL. Harvesting low-frequency (<5 Hz) irregular mechanical energy: a possible killer application of triboelectric nanogenerator. *ACS Nano*. 2016;10(4):4797-4805. https://doi.org/10.1021/acsnano.6b01569.
82. Pu X, Guo H, Chen J, et al. Eye motion triggered self-powered mechnosensational communication system using triboelectric nanogenerator. *Sci Adv*. 2017;3(7):e1700694. https://doi.org/10.1126/sciadv.1700694.
83. Jin L, Tao J, Bao R, Sun L, Pan C. Self-powered real-time movement monitoring sensor using triboelectric nanogenerator technology. *Sci Rep*. 2017;7(1):10521. https://doi.org/10.1038/s41598-017-10990-y.
84. Wang X, Yang Y. Effective energy storage from a hybridized electromagnetic-triboelectric nanogenerator. *Nano Energy*. 2017;32:36-41. https://doi.org/10.1016/j.nanoen.2016.12.006.
85. Chen J, Pu X, Guo H, et al. A self-powered 2D barcode recognition system based on sliding mode triboelectric nanogenerator for personal identification. *Nano Energy*. 2018;43:253-258. https://doi.org/10.1016/j.nanoen.2017.11.028.
86. Wang J, Ding W, Pan L, et al. Self-powered wind sensor system for detecting wind speed and direction based on a Triboelectric Nanogenerator. *ACS Nano*. 2018;12(4):3954-3963. https://doi.org/10.1021/acsnano.8b01532.
87. Jiang Q, Chen B, Zhang K, Yang Y. Ag nanoparticle-based triboelectric nanogenerator to scavenge wind energy for a self-charging power unit. *ACS Appl Mater Interfaces*. 2017;9(50):43716-43723. https://doi.org/10.1021/acsami.7b14618.
88. Xing F, Jie Y, Cao X, Li T, Wang N. Natural triboelectric nanogenerator based on soles for harvesting low-frequency walking energy. *Nano Energy*. 2017;42:138-142. https://doi.org/10.1016/j.nanoen.2017.10.029.
89. Wang S, Niu S, Yang J, Lin L, Wang ZL. Quantitative measurements of vibration amplitude using a contact-mode free-standing triboelectric nanogenerator. *ACS Nano*. 2014;8(12):12004-12013. https://doi.org/10.1021/nn5054365.
90. Wang S, Xie Y, Niu S, Lin L, Wang ZL. Freestanding Triboelectric-layer-based nanogenerators for harvesting energy from a moving object or human motion in contact and non-contact modes. *Adv Mater*. 2014;26(18):2818-2824. https://doi.org/10.1002/adma.201305303.
91. Zi Y, Wang J, Wang S, et al. Effective energy storage from a triboelectric nanogenerator. *Nat Commun*. 2016;7:10987. https://doi.org/10.1038/ncomms10987.
92. Guo H, Pu X, Chen J, et al. A highly sensitive, self-powered triboelectric auditory sensor for social robotics and hearing aids. *Sci Robot*. 2018;3(20):eaat2516. https://doi.org/10.1126/scirobotics.aat2516.
93. Zhu G, Chen J, Zhang T, Jing Q, Wang ZL. Radial-arrayed rotary electrification for high performance triboelectric generator. *Nat Commun*. 2014;5(1):3426. https://doi.org/10.1038/ncomms4426.
94. Wen Z, Chen J, Yeh M-H, et al. Blow-driven triboelectric nanogenerator as an active alcohol breath analyzer. *Nano Energy*. 2015;16:38-46. https://doi.org/10.1016/j.nanoen.2015.06.006.
95. Zheng H, Zi Y, He X, et al. Concurrent harvesting of ambient energy by hybrid Nanogenerators for wearable self-powered systems and active remote sensing. *ACS Appl Mater Interfaces*. 2018;10(17):14708-14715. https://doi.org/10.1021/acsami.8b01635.
96. Wang Y, Yang Y, Wang ZL. Triboelectric nanogenerators as flexible power sources. *Npj Flex Electron*. 2017;1(1):10. https://doi.org/10.1038/s41528-017-0007-8.
97. Ahmed A, Saadatnia Z, Hassan I, et al. Self-powered wireless sensor node enabled by a duck-shaped triboelectric nanogenerator for harvesting water wave energy. *Adv Energy Mater*. 2017;7(7):1601705. https://doi.org/10.1002/aenm.201601705.
98. Jing Q, Zhu G, Wu W, et al. Self-powered triboelectric velocity sensor for dual-mode sensing of rectified linear and rotary motions. *Nano Energy*. 2014;10:305-312. https://doi.org/10.1016/j.nanoen.2014.09.018.
99. Zheng Q, Shi B, Fan F, et al. In vivo powering of pacemaker by breathing-driven implanted triboelectric nanogenerator. *Adv Mater*. 2014;26(33):5851-5856. https://doi.org/10.1002/adma.201402064.
100. Ouyang H, Tian J, Sun G, et al. Self-powered pulse sensor for antidiastole of cardiovascular disease. *Adv Mater*. 2017;29(40):1703456. https://doi.org/10.1002/adma.201703456.
101. Kim H-J, Kim J-H, Jun K-W, et al. Silk nanofiber-networked bio-triboelectric generator: silk bio-TEG. *Adv Energy Mater*. 2016;6(8):1502329. https://doi.org/10.1002/aenm.201502329.
102. Liu G, Nie J, Han C, et al. Self-powered electrostatic adsorption face mask based on a triboelectric nanogenerator. *ACS Appl Mater Interfaces*. 2018;10(8):7126-7133. https://doi.org/10.1021/acsami.7b18732.
103. Yang Y, Zhang H, Zhong X, et al. Electret film-enhanced triboelectric nanogenerator matrix for self-powered instantaneous tactile imaging. *ACS Appl Mater Interfaces*. 2014;6(5):3680-3688. https://doi.org/10.1021/am406018h.
104. Zhang J, Zheng Y, Xu L, Wang D. Oleic-acid enhanced triboelectric nanogenerator with high output performance and wear resistance. *Nano Energy*. 2020;69:104435. https://doi.org/10.1016/j.nanoen.2019.104435.
105. Yong H, Chung J, Choi D, Jung D, Cho M, Lee S. Highly reliable wind-rolling triboelectric nanogenerator operating in a wide wind speed range. *Sci Rep*. 2016;6(1):33977. https://doi.org/10.1038/srep33977.
106. Zhang L, Zhang B, Chen J, et al. Lawn structured triboelectric nanogenerators for scavenging sweeping wind energy on rooftops. *Adv Mater*. 2016;28(8):1650-1656. https://doi.org/10.1002/adma.201504462.
107. Cui N, Liu J, Gu L, Bai S, Chen X, Qin Y. Wearable triboelectric generator for powering the portable electronic devices. *ACS Appl Mater Interfaces*. 2015;7(33):18225-18230. https://doi.org/10.1021/am5071688.
108. Zhou T, Zhang C, Han CB, Fan FR, Tang W, Wang ZL. Woven structured triboelectric nanogenerator for wearable devices. *ACS Appl Mater Interfaces*. 2014;6(16):14695-14701. https://doi.org/10.1021/am504110u.
109. Lin Z, Yang J, Li X, et al. Large-scale and washable smart textiles based on triboelectric nanogenerator arrays for self-powered sleeping monitoring. *Adv Funct Mater*. 2018;28(1):1704112. https://doi.org/10.1002/adfm.201704112.

110. Li S, Wang J, Peng W, et al. Sustainable energy source for wearable electronics based on multilayer elastomeric triboelectric nanogenerators. *Adv Energy Mater*. 2017;7:1602832. https://doi.org/10.1002/aenm.201602832.
111. Lai Y-C, Deng J, Zhang SL, Niu S, Guo H, Wang ZL. Single-thread-based wearable and highly stretchable Triboelectric Nanogenerators and their applications in cloth-based self-powered human-interactive and biomedical sensing. *Adv Funct Mater*. 2017;27(1):1604462. https://doi.org/10.1002/adfm.201604462.
112. Tian Z, He J, Chen X, et al. Core–shell coaxially structured triboelectric nanogenerator for energy harvesting and motion sensing. *RSC Adv*. 2018;8(6):2950-2957. https://doi.org/10.1039/C7RA12739A.
113. Jiang Q, Wu C, Wang Z, et al. MXene electrochemical microsupercapacitor integrated with triboelectric nanogenerator as a wearable self-charging power unit. *Nano Energy*. 2018;45:266-272. https://doi.org/10.1016/j.nanoen.2018.01.004.
114. Kim H-J, Yim E-C, Kim J-H, Kim S-J, Park J-Y, Oh I-K. Bacterial nano-cellulose triboelectric nanogenerator. *Nano Energy*. 2017;33:130-137. https://doi.org/10.1016/j.nanoen.2017.01.035.
115. Liang Q, Zhang Q, Yan X, et al. Recyclable and green triboelectric nanogenerator. *Adv Mater*. 2017;29(5):1604961. https://doi.org/10.1002/adma.201604961.
116. Chen S, Jiang J, Xu F, Gong S. Crepe cellulose paper and nitrocellulose membrane-based triboelectric nanogenerators for energy harvesting and self-powered human-machine interaction. *Nano Energy*. 2019;61:69-77. https://doi.org/10.1016/j.nanoen.2019.04.043.
117. Kim S, Gupta MK, Lee KY, et al. Transparent flexible graphene triboelectric nanogenerators. *Adv Mater*. 2014;26(23):3918-3925. https://doi.org/10.1002/adma.201400172.
118. Yi F, Wang X, Niu S, et al. A highly shape-adaptive, stretchable design based on conductive liquid for energy harvesting and self-powered biomechanical monitoring. *Sci Adv*. 2016;2(6):e1501624. https://doi.org/10.1126/sciadv.1501624.
119. Ryu H, Lee J-H, Kim T-Y, et al. High-performance triboelectric nanogenerators based on solid polymer electrolytes with asymmetric pairing of ions. *Adv Energy Mater*. 2017;7(17):1700289. https://doi.org/10.1002/aenm.201700289.
120. Yao C, Yin X, Yu Y, Cai Z, Wang X. Chemically functionalized natural cellulose materials for effective triboelectric nanogenerator development. *Adv Funct Mater*. 2017;27(30):1700794. https://doi.org/10.1002/adfm.201700794.
121. Wu C, Kim TW, Park JH, et al. Enhanced triboelectric nanogenerators based on MoS 2 monolayer nanocomposites acting as electron-acceptor layers. *ACS Nano*. 2017;11(8):8356-8363. https://doi.org/10.1021/acsnano.7b03657.
122. Seol M, Kim S, Cho Y, et al. Triboelectric series of 2D layered materials. *Adv Mater*. 2018;30(39):1801210. https://doi.org/10.1002/adma.201801210.
123. Zi Y, Niu S, Wang J, Wen Z, Tang W, Wang ZL. Standards and figure-of-merits for quantifying the performance of triboelectric nanogenerators. *Nat Commun*. 2015;6(1):8376. https://doi.org/10.1038/ncomms9376.
124. Zhang R, Hummelgård M, Örtegren J, et al. Human body constituted triboelectric nanogenerators as energy harvesters, code transmitters, and motion sensors. *ACS Appl Energy Mater*. 2018;1(6):2955-2960. https://doi.org/10.1021/acsaem.8b00667.
125. Zhang R, Dahlström C, Zou H, et al. Cellulose-based fully green triboelectric nanogenerators with output power density of 300 W m−2. *Adv Mater*. 2020;2002824:1-8. https://doi.org/10.1002/adma.202002824.
126. Liu T, Liu M, Dou S, et al. Triboelectric-nanogenerator-based soft energy-harvesting skin enabled by toughly bonded elastomer/hydrogel hybrids. *ACS Nano*. 2018;12(3):2818-2826. https://doi.org/10.1021/acsnano.8b00108.
127. Yang H, Fan FR, Xi Y, Wu W. Bio-derived natural materials based Triboelectric devices for self-powered ubiquitous wearable and implantable intelligent devices. *Adv Sustain Syst*. 2020;4:2000108. https://doi.org/10.1002/adsu.202000108.
128. Kim JN, Lee J, Go TW, et al. Skin-attachable and biofriendly chitosan-diatom triboelectric nanogenerator. *Nano Energy*. 2020;75:104904. https://doi.org/10.1016/j.nanoen.2020.104904.
129. Wang R, Gao S, Yang Z, et al. Engineered and laser-processed chitosan biopolymers for sustainable and biodegradable triboelectric power generation. *Adv Mater*. 2018;30(11):1-8. https://doi.org/10.1002/adma.201706267.
130. Bao Y, Wang R, Lu Y, Wu W. Lignin biopolymer based triboelectric nanogenerators. *APL Mater*. 2017;5(7):074109. https://doi.org/10.1063/1.4984625.
131. Han Y, Han Y, Zhang X, et al. Fish gelatin based triboelectric nanogenerator for harvesting biomechanical energy and self-powered sensing of human physiological signals. *ACS Appl Mater Interfaces*. 2020;12(14):16442-16450. https://doi.org/10.1021/acsami.0c01061.
132. An S, Sankaran A, Yarin AL. Natural biopolymer-based triboelectric nanogenerators via fast, facile, scalable solution blowing. *ACS Appl Mater Interfaces*. 2018;10(43):37749-37759. https://doi.org/10.1021/acsami.8b15597.
133. Wang W, Zhang J, Zhang Y, et al. Remarkably enhanced hybrid piezo/triboelectric nanogenerator via rational modulation of piezoelectric and dielectric properties for self-powered electronics. *Appl Phys Lett*. 2020;116(2):023901. https://doi.org/10.1063/1.5134100.
134. Nie S, Fu Q, Lin X, Zhang C, Lu Y, Wang S. Enhanced performance of a cellulose nanofibrils-based triboelectric nanogenerator by tuning the surface polarizability and hydrophobicity. *Chem Eng J*. 2021;404:126512. https://doi.org/10.1016/j.cej.2020.126512.
135. Zhang C, Lin X, Zhang N, et al. Chemically functionalized cellulose nanofibrils-based gear-like triboelectric nanogenerator for energy harvesting and sensing. *Nano Energy*. 2019;66:104126. https://doi.org/10.1016/j.nanoen.2019.104126.
136. Kim YJ, Lee J, Park S, Park C, Park C, Choi H-J. Effect of the relative permittivity of oxides on the performance of

triboelectric nanogenerators. *RSC Adv*. 2017;7(78):49368-49373. https://doi.org/10.1039/C7RA07274K.

137. Gu GQ, Han CB, Tian JJ, et al. Antibacterial composite film-based triboelectric nanogenerator for harvesting walking energy. *ACS Appl Mater Interfaces*. 2017;9(13):11882-11888. https://doi.org/10.1021/acsami.7b00230.
138. Kim M-K, Kim M-S, Kwon H-B, Jo S-E, Kim Y-J. Wearable triboelectric nanogenerator using a plasma-etched PDMS–CNT composite for a physical activity sensor. *RSC Adv*. 2017;7(76):48368-48373. https://doi.org/10.1039/C7RA07623A.
139. Cheon S, Kang H, Kim H, et al. High-performance triboelectric nanogenerators based on electrospun Polyvinylidene fluoride-silver nanowire composite Nanofibers. *Adv Funct Mater*. 2018;28(2):1703778. https://doi.org/10.1002/adfm.201703778.

AUTHOR BIOGRAPHY

Renyun Zhang is an associate professor at Mid Sweden University. He received his PhD in 2007 in Biomedical Engineering at Southeast University, and then spent 3 years as a postdoctoral research fellow at Mid Sweden University. His research focuses on the energy harvesting technology and transparent thin films.

How to cite this article: Zhang R, Olin H. Material choices for triboelectric nanogenerators: A critical review. *EcoMat*. 2020;2:e12062. https://doi.org/10.1002/eom2.12062